Science Translational Medicine
AAAS

stm.sciencemag.org/cgi/content/full/12/553/eaaw0638/DC1

Supplementary Materials for

Apoptosis of hematopoietic progenitor-derived adipose tissue–resident macrophages contributes to insulin resistance after myocardial infarction

Sathish Babu Vasamsetti, Emilie Coppin, Xinyi Zhang, Jonathan Florentin, Sasha Koul, Matthias Götberg, Andrew S. Clugston, Floyd Thoma, John Sembrat, Grant C. Bullock, Dennis Kostka, Claudette M. St. Croix, Ansuman Chattopadhyay, Mauricio Rojas, Suresh Mulukutla, Partha Dutta*

*Corresponding author. Email: duttapa@pitt.edu

Published 22 July 2020, *Sci. Transl. Med.* **12**, eaaw0638 (2020)
DOI: 10.1126/scitranslmed.aaw0638

The PDF file includes:

Legends for movies S1 and S2

Other Supplementary Material for this manuscript includes the following:

(available at stm.sciencemag.org/cgi/content/full/12/553/eaaw0638/DC1)

Movies S1 and S2 (.mp4 format). MI decreases the frequency of VAT-resident macrophages.
Data file S1 (Microsoft Excel format).

MATERIALS AND METHODS

Mouse models of cellular fate mapping

To investigate the origin of adipose tissue macrophages, we used Csf1r-mer-cre-mer (Jackson Lab, #019098), *Cx$_3$cr1*^{creER} (Jackson Lab, #021160), ROSA-tdTomato (Jackson Lab, #007914) and Flt3^{creER} (a gift from Dr. Jean Valmier). Female ROSA-tdTomato mice were mated with either male Csf1r-mer-cre-mer, *Cx$_3$cr1*^{creER} or Flt3^{creER} mice. We injected tamoxifen (50 µl of 20 mg/ ml solution, Sigma, T5648) and progesterone (50 µl of 10 mg/ ml solution, Sigma, P0130) dissolved in corn oil (Sigma, C8267) in pregnant female mice at various timepoints to induce permanent tdTomato expression in progenitor or precursor cells expressing the transgenes at the time of the injection. The offspring were only injected with tamoxifen at time points after birth. The progenies derived from these labelled cells express tdTomato even though they lose the expression of the transgenes. To assess the contributions of yolk sac progenitors and pre-macrophages in the origin of adipose macrophages, we injected tamoxifen and progesterone at embryonic day 8.5 (E8.5) and E13, respectively, in the pregnant mice. Tamoxifen (20 µl of 20 mg/ ml solution) was injected at post-partum day 0 (P0) in Flt3^{creER}-tdTomato offspring to understand the differentiation ability of hematopoietic progenitors into adipose macrophages. tdTomato expression in adipose macrophages was determined using flow cytometry and confocal microscopy.

Myocardial infarction

Mice were anesthetized and left thoracic and abdominal regions of the mouse were shaved and cleaned with butadiene scrub. The mouse was intubated using a laryngoscope and a 22-gauge angiocatheter sheath and ventilated by Harvard ventilator. The mouse was placed on a heating pad, and a thoracotomy was performed between the 3rd and 4th intercostal space. We ligated the

left anterior descending (LAD) coronary artery with 8-0 suture. Two separate 5-0 sutures were used to close the rib cage. The skin was sutured using a 5-0 suture, and air was removed from thoracic cavity via a catheter sheath and a 3 mL syringe. Animals were extubated when spontaneous breathing resumed. We injected buprenorphine just after coronary ligation and before suturing the thorax, tracheal extubation and isoflurane withdrawal. The mice normally woke up 20-30 minutes after buprenorphine injection. We continued buprenorphine injection for 3 days after the surgery. Mice were monitored by veterinarians daily for any signs of pain after a surgical procedure. If any mice did not exhibit normal recovery after surgery, we euthanized them after consulting with veterinarians.

Skeletal muscle injury

To induce skeletal muscle injury, mice were injected with 100 µl of 0.6% barium chloride ($BaCl_2$) in the tibialis anterior muscles for three days.

Parabiosis

Post anesthesia, adjacent sides of $CX_3CR1^{+/GFP}$ $CD45.2^{+}$ and $CX_3CR1^{+/+}$ CD45.1 mice were sterilized with butadiene scrub followed by 70% isopropanol. The mouse was placed on a heating pad, and an incision was made from the ear to the tail of each mouse. The subcutaneous fascia was bluntly dissected to create about 1/2 cm of free skin. The olecranon and knee joints were attached by a single 2-0 silk suture and tied. The skin of the mice was joined together using a 5-0 suture. Stifle and elbows were joined to avoid stress on the suture lines. Non-absorbable sutures were removed on day 7 after the surgery.

Intravital microscopy

$CX_3CR1^{CreER/+}$ $ROSA^{tdTomato/+}$ mice were injected daily with 100 µl of 20 mg/ml of tamoxifen (Sigma) dissolved in corn oil (Sigma) for five consecutive days. After disinfecting the abdominal

region using butadiene scrub and 70% ethanol, a part of gonadal adipose tissue was taken out of the abdomen and imaged after placing it in sterile 0.9% saline to prevent dehydration using a two photon microscope. The microscope was equipped with a heated mouse holder to maintain a body temperature of 37^{o} C. Over the duration of imaging, Methocel 2% gel was used to avoid dehydration of the tissue and maintain contact between the tissue and the microscope objective. The total imaging duration was 30-60 minutes per mouse. Data analysis was performed using ImageJ software.

Histology and immunofluorescence microscopy

Following euthanization of mice and 20 ml PBS perfusion through the left ventricle, visceral adipose tissue, brain and liver were excised and fixed with 4% buffered formalin for 2 hours and stored in 30% sucrose solution containing 0.05% sodium azide for overnight. For immunofluorescence staining, tissue sections were permeabilized with 0.1% triton X-100 for an hour. After blocking, mouse tissue sections were stained with anti-F4/80 (clone A3-1, Invitrogen, MAI-91124), CD 11b (EPR1344, Abcam, ab133357) followed by staining with fluorochrome conjugated secondary antibodies. The sections were stained and fixed with Vectashield mounting medium with DAPI (Vector Laboratories), and images were taken using confocal laser scanning immunofluorescence microscopy. Image analysis was done using ImageJ software. After excision, aortic roots were embedded in OCT blocks, and aortic root sections (5 μm) were stained with Masson's trichrome to assess plaque size and fibrous cap thickness.

Organ harvesting, flow cytometry and cell sorting

Mice were euthanized and perfused thoroughly with 30 mL of ice cold PBS through the left ventricle to remove blood from solid organs. Gonadal and mesenteric adipose tissue, brain and liver were harvested and digested in PBS containing 1 mg/ml of collagenase IV (Worthington)

and 20 μM HEPES buffer at 37° C on thermoblock by rotating at 750 rpm for 40 minutes. Aortae were excised and digested in enzymatic mixture containing 450 U/ml collagenase I (Sigma, C0130), 125 U/ml collagenase XI (Sigma), 60 U/ml DNase I (Worthington), and 60 U/ml hyaluronidase (Sigma) at 37°C at 750 rpm for 40 minutes. After red blood cell lysis for three minutes using RBC lysis buffer (BioLegend), blood cells were washed and resuspended in cold FACS buffer (PBS containing 0.5% BSA). Cell staining and analysis were performed as described previously (*33*). All antibodies used in this study were purchased from eBioscience, BioLegend and BD Biosciences. All of the antibodies except anti-CCR2 antibodies were used in 1:600 dilutions for flow cytometry staining. Anti-mouse and human CCR2 antibodies were used in 1:30 dilutions. For leukocyte and progenitor cell analyses in mice, monoclonal antibodies including anti-CD11b (M1/70, BD Biosciences), CD 11c (HL3, BD Biosciences), Ly6G (1A8, BioLegend), CD115 (AFS98, eBioscience), Ly-6C (HK 1.4, eBioscience), CD19 (1D3, BD Biosciences), MHC class II (M5/114.15.2 eBioscience), CD64 (X54-5/7.1, BD Biosciences), F4/80 (BM8, BioLegend), CD45.1 (A20, BioLegend), CD45.2 (104, BioLegend), C-kit (2B8, BioLegend), CCR2 (R&D Systems) and streptavidin (BD Biosciences) were used. Neutrophils were identified as $CD11b^+$ $Ly6G^+$, and monocytes were defined as $CD11b^+$ $CD115^+$. Macrophages were considered as $CD45^+$ $CD11b^+$ $CD64^+$ $F4/80^+$. The gating strategy for $CCR2^+$ macrophages was adjusted based on the CCR2 staining in $CCR2^{-/-}$ mice. Pre-macrophages were identified as $F4/80^-$ $CD11b^-$ CX_3CR1^+ $CD45^+$ $C\text{-}kit^+$. Human omental leukocytes were stained with antibodies against CD45 (HI30, BD Biosciences), CCR2 (K036C2, BioLegend), CD24 (ML5, BD Biosciences), CD14 (HCD 14, BioLegend), CD16 (3G8, BD Biosciences), CD11c (B-ly6, BD Biosciences), CD 206 (19.2, BD Biosciences), and HLA-DR (G46-6, BD Biosciences). Human adipose tissue macrophages were identified as $CD45^+$ $CD11c^+$ $CD206^+$.

Data acquisition was performed using a Fortessa Flow Cytometer (BD). Data were analyzed using FlowJo software (Tree Star). Apoptosis of cells by flow was measured using FITC Annexin V apoptosis detection I and PE- active Caspase 3 apoptosis kits from BD Biosciences.

Whole-mount imaging of VAT using confocal microscopy

VAT tissue was fixed with formalin and incubated in 30% sucrose solution containing 0.05% sodium azide incubated. VAT tissues were cut into small pieces of 0.1 cm size and permeabilized with 0.1% triton X-100 for 4 hours. Tissue sections were blocked for overnight in PBS containing 2% BSA and stained with primary antibodies like F4/80 (A3-1, Invitrogen, MAI-91124), cleaved caspase 3 (Abcam, ab13847), CD11b (EPR1344, Abcam, ab133357), M-CSF1 (M-CSF1 ELISA kit, Thermofisher, EMCSF1) for 48 hours followed by washing with PBS and incubation with fluorochrome conjugated secondary antibodies for 24 hours at 4°C. Tissue sections were stained and mounted with Vectashield DAPI, and images were taken using confocal laser microscopy and analyzed using image J. Apoptotic cells were detected by measuring TUNEL positive cells in the VAT whole mount tissue by using Sigma In Situ Cell Death Detection (TUNEL) Kit, Fluorescein (11684795910). To detect necroptotic macrophages, we used anti-pMLKL (phospho S345) antibody (EPR9515(2), Abcam, ab196436).

In vivo administration of M-CSF

Following MI surgery by ligation of the coronary artery, mice were injected with 100 µl of either sterile PBS or PBS containing 1.68 IUx10^5 units/ µg of M-CSF (R&D Systems, 216-MC-025 µg) / day for 5 days i.p.

Treatment with clodronate (dichloromethylenediphosphonic acid) liposome

After MI, mice were injected with 100 mg/kg body weight of either control or clodronate liposome (Encapsula Nanosciences) dissolved in 200 µl of sterile PBS i.p. For a different set of

experiments, we have also injected either with 100 mg/ kg of control or clodronate liposome directly in different parts of gonadal adipose tissue. To this end, we exposed gonadal adipose tissue after a small incision on the lower linea alba. Control or clodronate liposome was injected in the adipose tissue. VAT was returned into the abdomen and the skin was sutured using a 5-0 nylon suture.

Depletion of VAT resident macrophages in *LysM*$^{cre/+}$ *ChR2*$^{fl/fl}$ mice

To induce apoptosis in VAT resident macrophages, we generated *LysM*$^{cre/+}$ ChR2$^{fl/fl}$ mice that express the channelrhodopsin-2 (ChR2) protein in macrophages. *Chlamydomonas reinhardtii*-derived ChR2 is composed of a blue light-sensitive domain with an ion channel, providing light-dependent ion transport and membrane potential. Illuminating ChR2-expressing macrophages with blue light (450-490 nm) leads to photostimulation of action potential and firing activity. Mice were anesthetized by injecting ketamine (100 mg/ kg body weight) combined with xylazine (10 mg/ kg body weight) i.p. A small incision was made on the abdominal skin, and epididymal adipose tissue was exposed. A small hole was made on a piece of aluminum foil, which was placed on a blue light source of the Light Box. The mouse was placed in such a way that the adipose tissue protruded through the hole. Other body parts were not exposed to the light. The mice were not placed on a heating bad during photostimulation. Epididymal adipose tissue was illuminated with blue light (440 nm) for 20 minutes. To understand the effect of VAT resident macrophages on MI-induced insulin resistance, this macrophage subset was depleted in *LysM*$^{cre/+}$ ChR2$^{fl/fl}$ mice with blue light one day after MI surgery. GTT and ex vivo analyses were performed six days later.

Glucose, insulin, and pyruvate tolerance tests

Mice were fasted for 6 hours and injected with 10% sterile glucose solution (2 g/kg body weight

dissolved in PBS) intraperitoneally after measuring fasting glucose contents. Blood samples were drawn by tail nick and glucose concentrations were measured at 15, 30, 60, 90, 120 and 150 minutes after glucose injection. For insulin tolerance test, after fasting for 6 hours, mice were injected with insulin (0.25 U/kg body weight) and blood glucose contents were measured at the various timepoints mentioned above. Sterile pyruvate solution (2 gm/ Kg body weight) was injected i.p for pyruvate tolerance test.

Estimation of serum insulin, catecholamine, cortisol, and adiponectin concentrations

In anaesthetized mice, blood was collected via either retro-orbital bleeding or cardiac puncture using non-heparin coated capillary tubes, and serum was separated by centrifugation (3000 rpm for 10 minutes at 4°C) and stored at -80°C until further analyses. Insulin concentrations were analyzed by using the ultrasensitive mouse insulin ELISA kit (Mercordia Diagnostics). M-CSF amounts were quantified using an M-CSF1 ELISA kit (Thermofisher). Serum Catecholamines were analyzed by using Epinephrine/Norepinephrine ELISA kit from (Abnova), and cortisol concentrations were measured using a cortisol ELISA kit (R&D). For adiponectin analysis, serum was 20,000 times diluted with ELISA dilution buffer, and 100 µl of diluted serum was loaded on ELISA coating plates. The assay was performed according to the manufacturer's instructions (Invitrogen).

Estimation of serum triglycerides, free fatty acids, and glycerol concentrations

Following serum separation, triglycerides were quantified in 5 µl of samples using Pointe Scientific triglyceride reagents. Free glycerol and free fatty acid were measured using EnzyChrom free glycerol assay kit (EGLY-200) and EnzyChrom free fatty acid assay kit (EFFA-100), respectively, from Bioassay Systems.

VAT transplantation

To harvest epididymal adipose tissue from donor *LysM*$^{cre/+}$ *Csf1r*$^{fl/fl}$ or *LysM*$^{+/+}$ *Csf1r*$^{fl/fl}$ mice, the mice were anesthetized using 1.5% isoflurane. The mice were shaved, and the surgical site was prepared with butadiene scrub followed by 70% ethanol. Mice were placed on a heating pad, to maintain body temperature during the procedure. A subcutaneous injection of buprenorphine (0.1mg/kg in a volume of 100 µl saline) was administered before the procedure. A laparotomy incision was made, and epididymal adipose tissue and blood vessels supplying this tissue were identified. The blood vessels were ligated using a 7-0 silk suture, and the adipose tissue was excised out. Recipient mice were prepared as the donor mice. Laparotomy incision were performed, and small pockets in epididymal adipose tissue of the recipient mice were created using a pair of blunt forceps. Donor adipose tissue was divided in several small parts and transplanted in the epididymal adipose tissue pockets without vascular anastomosis. The transplanted adipose tissue was secured using a 5-0 absorbable suture. Surgical wound was closed using a 5-0 suture. Mice were divided into the following experimental groups: A) *LysM*$^{+/+}$ *Csf1r*$^{fl/fl}$ adipose tissue into *LysM*$^{+/+}$ *Csf1r*$^{fl/fl}$ mice, B) *LysM*$^{cre/+}$ *Csf1r*$^{fl/fl}$ adipose tissue into *LysM*$^{cre/+}$ *Csf1r*$^{fl/fl}$ mice and C) *LysM*$^{+/+}$ *Csf1r*$^{fl/fl}$ adipose tissue into *LysM*$^{cre/+}$ *Csf1r*$^{fl/fl}$ mice. MI was induced in these mice 10 days after adipose tissue transplantation, and glucose tolerance test was performed 17 days after the transplantation.

Cell sorting and quantitative RT-PCR

To measure the mRNA of cytokines, we isolated stained single cell suspensions of adipose tissue as described above. VAT macrophage subsets were sorted using a FACS Aria, directly into 100 µl of RNA extraction buffer and stored in -80^{o}C freezer. mRNA was extracted, cDNA was made, and mRNA of cytokines was quantified with quantitative RT-PCR using the primers mentioned in table S2. Gene expression was expressed as Ct values normalized to the

housekeeping gene GAPDH. Heat maps were generated using Morpheus and Excel. For quantification of lipid metabolism genes in the liver, mRNA was extracted from the liver from mice after 16 hours of fasting.

pAkt measurement using immunoblotting

Following perfusion and euthanization of mice, the liver and quadriceps muscle were harvested and snap frozen in liquid N_2. Tissues were homogenized in RIPA (Alfa Aesar) lysis buffer containing phosphatase (Roche) and protease (Pierce) inhibitors. Homogenates were subjected to SDS-PAGE and blots were probed with primary antibodies for phosphorylated Akt (CST technologies, 4060) and total Akt (CST technologies, 4691). Subsequently, we incubated the blots with secondary IgG-HRP antibody, and images were captured by molecular imaging system as described previously.

Liver lipid extraction and quantification

Triglycerides were extracted from liver tissue using Nonide P 40 Substitute (Sigma- Aldrich Corp.). Liver tissue was homogenized with Nonidet P 40 Substitute, heated at 90 °C and chilled on ice. This procedure was repeated once, and subsequently insoluble materials were removed by centrifugation. Cholesterol was extracted from liver tissue by the Folch extraction method. Triglycerides and cholesterol concentrations were determined by enzymatic colorimetric assays.

Enumeration of apoptosis in VAT resident macrophages

Single cells obtained after VAT digestion were cultured in 1 ml DMEM containing 20 μM camptothecin (Sigma) for 3 hours to induce apoptosis. After this, the cells were stained for leukocyte markers. Annexin V and PI staining was performed following manufacturer's protocol using FITC Annexin V Apoptosis Kit (BD Biosciences).

BMDM culture, HMGB1 treatment, and TLR4, RAGE and NLRP3 silencing

Bone marrow cells were isolated from the femurs and tibias of PBS-perfused wild type C57BL/6 mice after euthanasia and cultured in DMEM (low glucose) containing 5.5 mM glucose and supplemented with 20% L929 conditioned medium. Cells were seeded in 12 well plates. After the cells were 80% confluent, the culture was treated with 0-1μg/ ml concentrations of recombinant mouse HMGB1 (BioLegend) for 16 hours and analyzed for apoptosis by using FITC Annexin V and PE- active Caspase 3 apoptosis kits from BD Biosciences. For gene silencing, cells were seeded in 6-well plates. We replaced the cell culture media with DMEM containing no FBS and antibiotics when the cells were 80% confluent. Then the cells were treated with 50 μl of OPTI-MEM (Gibco) containing 3 μl of Lipofectamine 2000 (Invitrogen) and 50 nM of either control, *Tlr4* or *Ager* siRNA (IDT). After 12 hours, cell culture medium was removed, and cells were incubated with DMEM medium containing L929-conditioned medium for 72 hours and treated with HMGB1 (1 μg/ml) for 16 hours before analysis.

RNASeq analysis

mRNA sequencing was performed by the Health Science Sequencing Core at UPMC Children Hospital of Pittsburgh. FASTQ files have been deposited to GSE118226. We used CLC Genomic Workbench to analyze RNAseq data. Briefly, we created QC report to check the quality of the data. Then, we trimmed off the adaptor sequences from the reads. The reads were mapped using a CLC reference for the mouse genome. After this, we calculated differential expression of genes using the software. We considered genes with FDR-corrected p value less than or equal to 0.05 as differentially expressed. PCA plots, Venn diagrams and heatmaps were generated for illustration purposes. Publicly available FASTQ files (GSE 81774 and GSE 99078)

were analyzed using CLC Genomic Workbench to compare transcriptional profile of various tissue resident macrophages. To identify VAT resident macrophage signature genes, we calculated the log2 fold change in VAT resident macrophages compared to microglia, Kupffer cells, and alveolar, skin, bone marrow and kidney macrophages. This analysis resulted in 93 genes, which were only expressed in VAT resident macrophages. For canonical pathway and transcription factor analyses, we used two independent software: Ingenuity Pathway Analysis (IPA) and BaseSpace Correlation Engine. Genes with at least 2-fold differences were selected for this purpose. We used BaseSpace Correlation Engine software to obtain common canonical pathways enriched in cardiac (GSE 53787) and VAT resident macrophages. Using IPA, we analyzed the 93 genes uniquely expressed by VAT resident macrophages and obtained genes and canonical pathways predicted to be differentially expressed in VAT resident macrophages compared to other tissue resident macrophages.

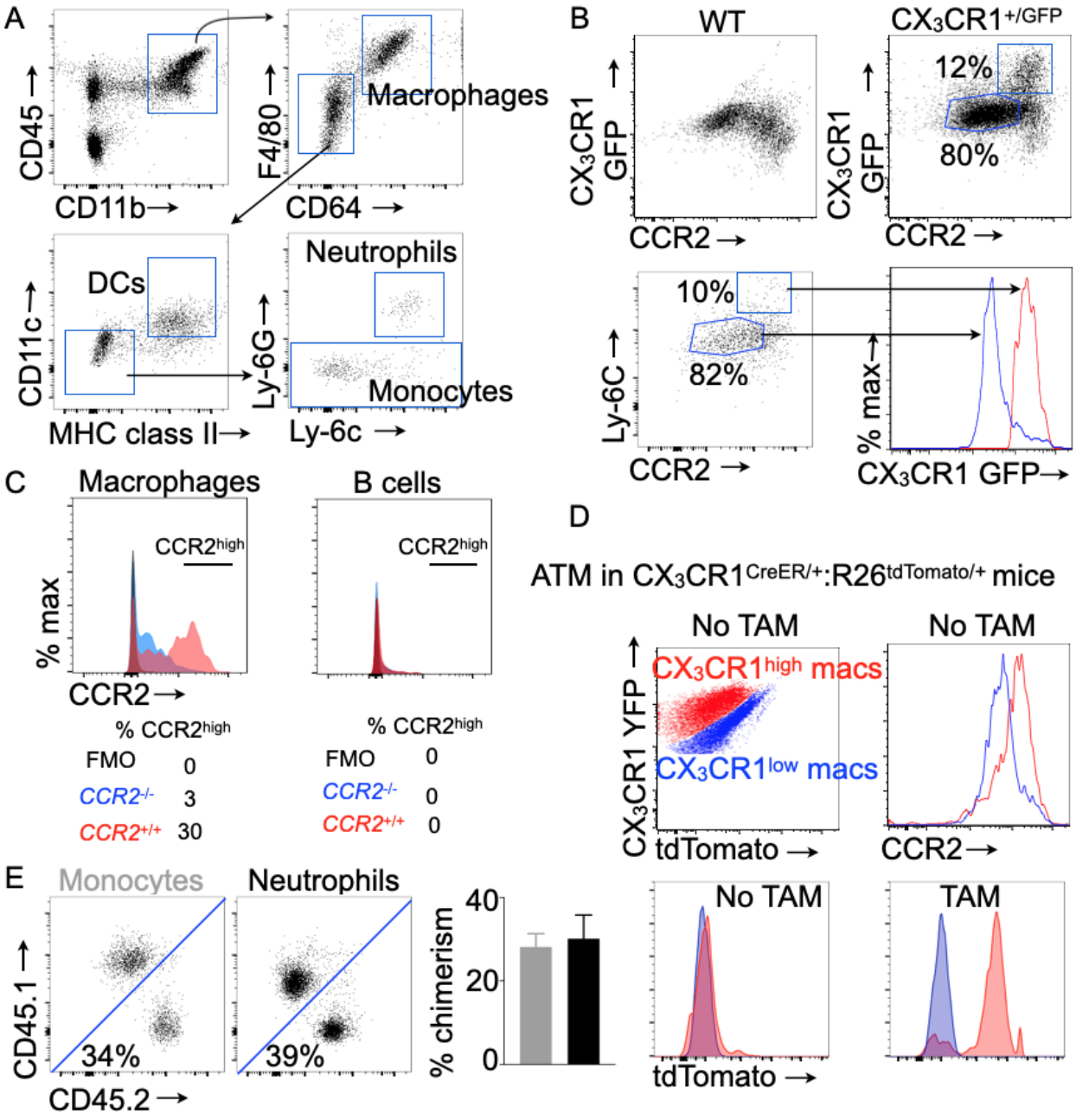

Fig. S1. CX$_3$CR1^{high} macrophages express CCR2 at high amounts. All of these experiments were performed in transgenic mice on a C57BL/6 background without MI. **(A)** Flow cytometric gating strategy for monocytes, macrophages, neutrophils and dendritic cells (DCs). VAT macrophages were identified as CD45$^+$ CD11b$^+$ F4/80$^+$ CD64$^+$. (**B**) VAT macrophage subsets in lean CX$_3$CR1$^{+/GFP}$ mice. (**C**) CCR2 or FMO staining was performed in VAT macrophages and B cells of wildtype and CCR2$^{-/-}$ mice. (**D**) VAT macrophage subsets were classified based on their CX$_3$CR1 expression in CX$_3$CR1$^{CreER/+}$ ROSA$^{tdTomato/+}$ mice after tamoxifen (TAM) injection. (**E**) Quantification of chimerism of CD45.2$^+$ circulating monocytes and neutrophils in CD45.1$^+$ mice two months after parabiosis between CX$_3$CR1$^{+/GFP}$ CD45.2 and CX$_3$CR1$^{+/+}$ CD45.1 mice. n=4 mice per group. Mean ± s.e.m.

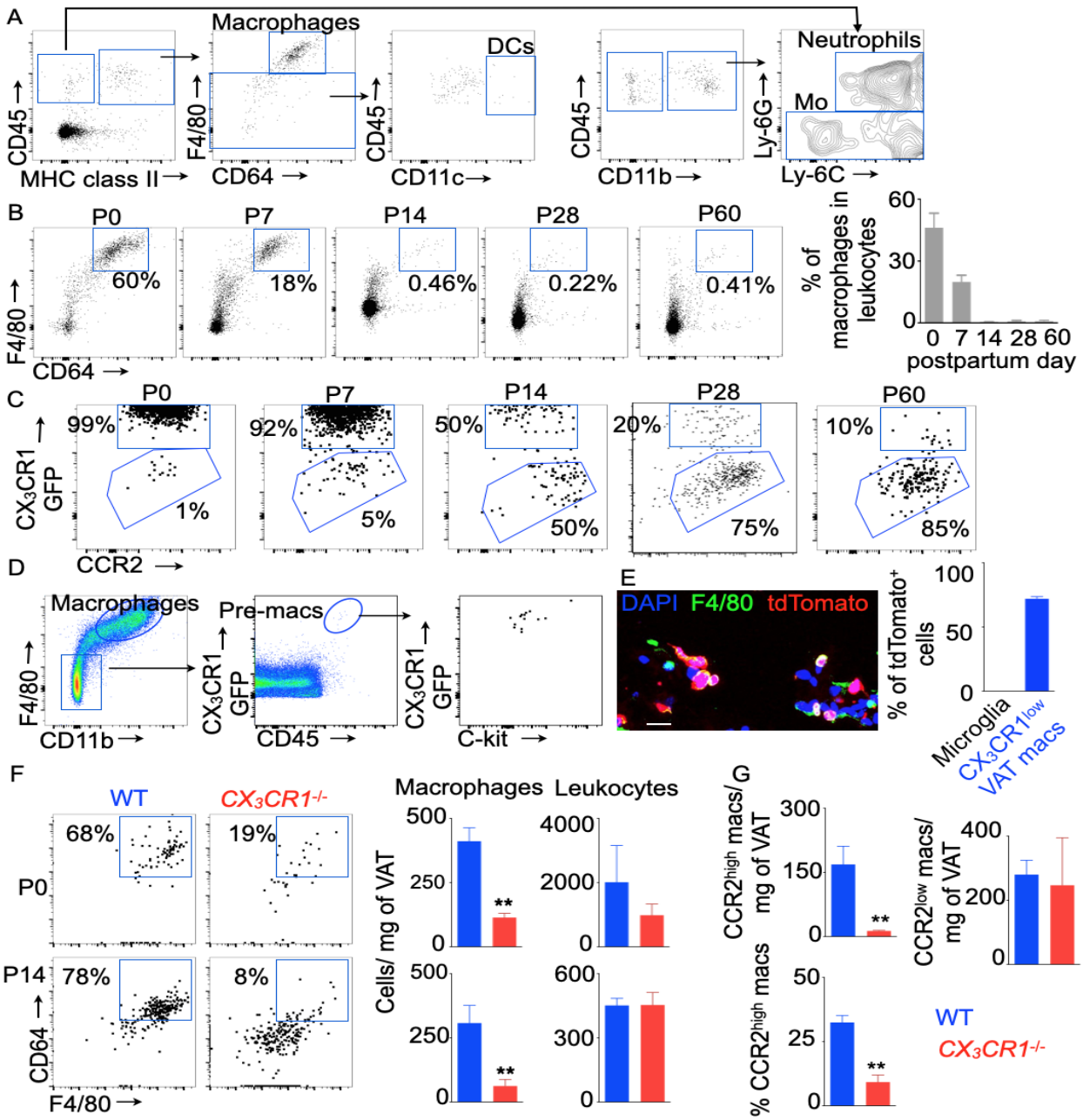

Fig. S2. VAT macrophage proportions gradually decrease after birth. All of these experiments were performed in lean transgenic mice on C57BL/6 background without MI. (**A**) Flow cytometric gating strategy for VAT myeloid cells on P0. (**B**) Quantification of macrophage frequency at various time points after birth. n=3-5 per group. (**C**) Flow cytometric plots show CX_3CR1^{high} and CX_3CR1^{low} macrophages at various timepoints after birth in $CX_3CR1^{+/GFP}$ mice. (**D**) Gating strategy for pre-macrophages in VAT of E13 embryos. n=7. (**E**) Tamoxifen was injected in Flt3-cre-YFP x ROSA-tdTomato offspring on P0, and $tdTomato^{+}$ VAT resident macrophages were enumerated using confocal microscopy on P28. Scale bar= 10 μm. n=4 for microglia and n=7 for CX_3CR1^{low} VAT macs. (**F&G**) Flow cytometric quantification of total macrophages, leukocytes and macrophage subsets in VAT of wild type and $CX_3CR1^{-/-}$ mice. n=5 per group for the P0 data, and n=4 for WT and n=10 for $CX_3CR1^{-/-}$ mice for the P14 data. Mean ± s.e.m. ** $P < 0.01$.

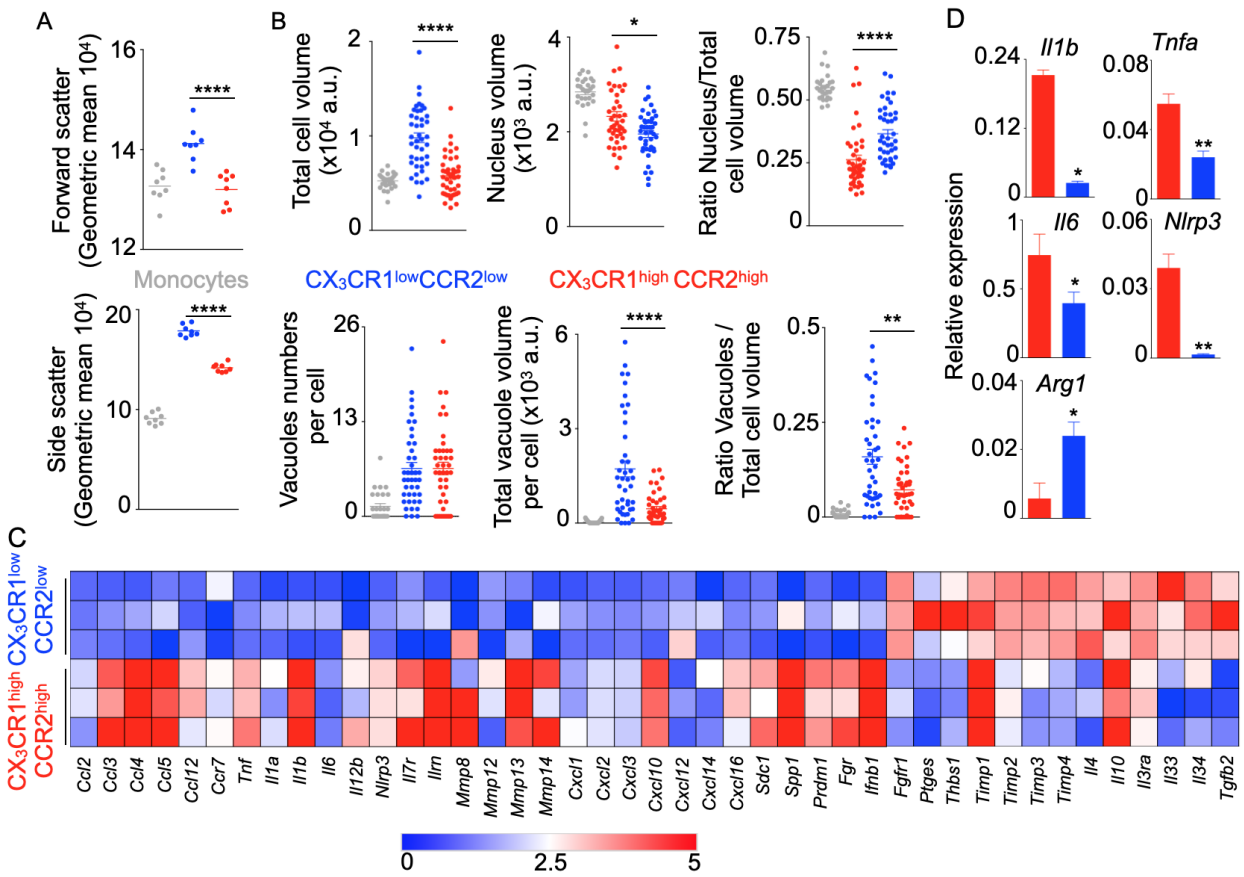

Fig. S3. CX₃CR1^{low} CCR2^{low} VAT-resident macrophages have a unique morphology compared to CX₃CR1^{high} CCR2^{high} VAT monocyte-derived macrophages and monocytes. All of these experiments were performed in lean C57BL/6 mice without MI. (**A**) Forward and side scatter profiles of blood monocytes and VAT macrophage subsets were determined by flow cytometry. (**B**) Different features of cell morphology were quantified by Wright-Giemsa staining. Data from two independently performed experiments are shown. (**C**) Inflammatory gene expression in the VAT macrophages. The list of ~~this~~ genes was obtained using Ingenuity Pathway Analysis of the RNA sequencing data comparing the two VAT macrophage subsets. (**D**) qPCR was performed to measure the relative expression of *Il1b*, *Il6* and *Arg1* in the VAT macrophage subsets. n=4-5 mice per group. Mean ± s.e.m. * P < 0.05, ** *P* < 0.01, **** *P* < 0.0001.

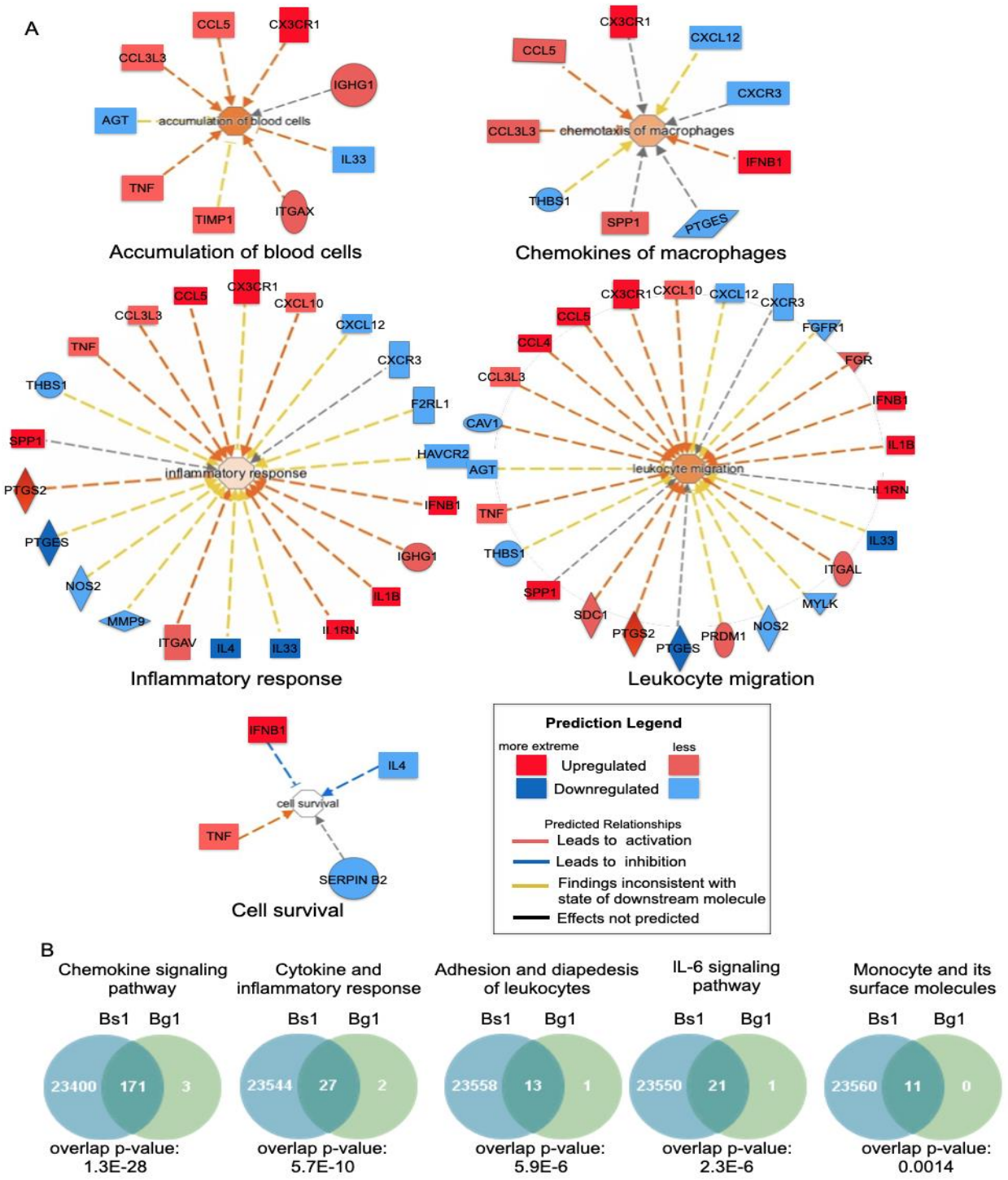

Fig. S4. CX_3CR1^{high} $CCR2^{high}$ VAT monocyte-derived macrophages are proinflammatory. All of these experiments were performed in lean C57BL/6 mice without MI. Analyses of RNA sequencing data using IPA (**A**) and BaseSpace Correlation Engine software (**B**) show the pathways enriched in CX_3CR1^{high} $CCR2^{high}$ VAT macrophages compared to CX_3CR1^{low} $CCR2^{low}$ VAT resident macrophages. In panel B, Bs1 represents enriched genes in CX_3CR1^{high} $CCR2^{high}$ vs. CX_3CR1^{low} $CCR2^{low}$ VAT resident macrophages, and Bg1 represents the genes in respective pathways.

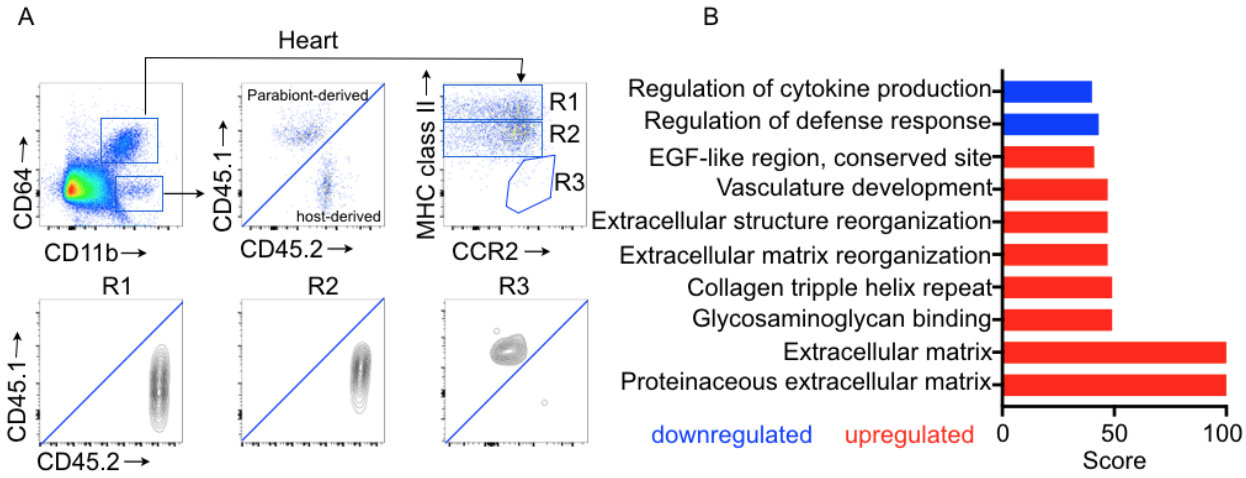

Fig. S5. VAT and cardiac resident macrophages have common canonical pathways. All of these experiments were performed in lean congenic mice on C57BL/6 background without MI. (**A**) Flow cytometric gating strategy for different cardiac macrophage subsets based on their MHC class II and CCR2 expression (upper panel). The middle and right flow cytometric plots of the upper panel show the chimerism in heart myeloid cells (without macrophages) and total macrophages, respectively, in CD45.2 parabionts six months after parabiosis. The lower panel shows the chimerism in different cardiac macrophage subsets of CD45.2 parabionts. (**B**) The bar graph shows the top ten pathways common between VAT (CX_3CR1^{low} $CCR2^{low}$) and cardiac (MHC class II^{high} $CCR2^{low}$) (GSE 53787) resident macrophages. This pathway analysis was performed using BaseSpace Correlation Engine software.

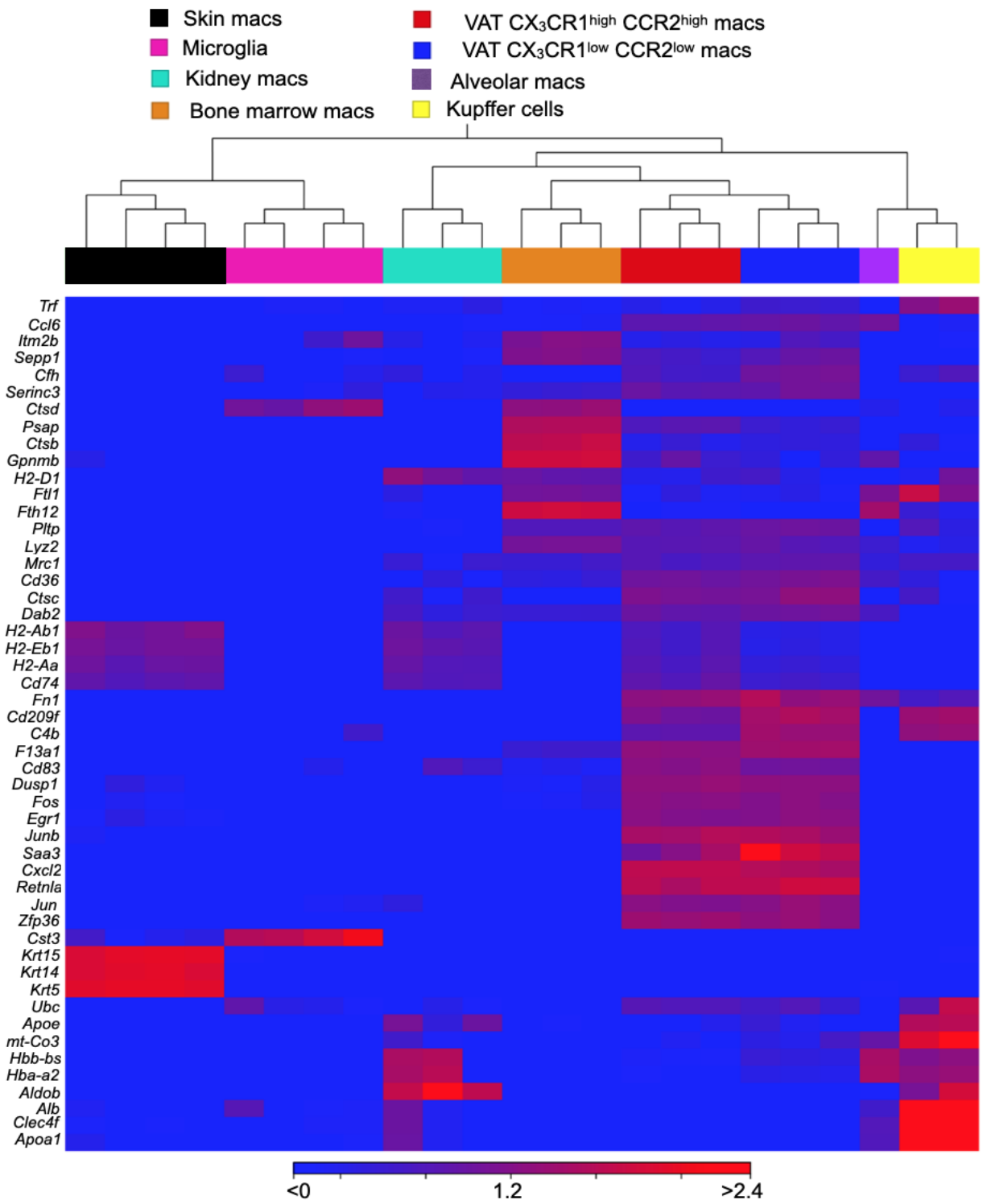

Fig. S6. CX_3CR1^{low} $CCR2^{low}$ VAT-resident macrophages express a unique transcriptional profile compared to other tissue-resident macrophages. All of these experiments were performed in lean C57BL/6 mice without MI. The transcriptome profile of the VAT macrophage subsets was compared to that of other tissue resident macrophages (GSE81774 and GSE99078) using CLC Genomics Workbench. The heat map shows 50 most differentially expressed genes among all tissue macrophages.

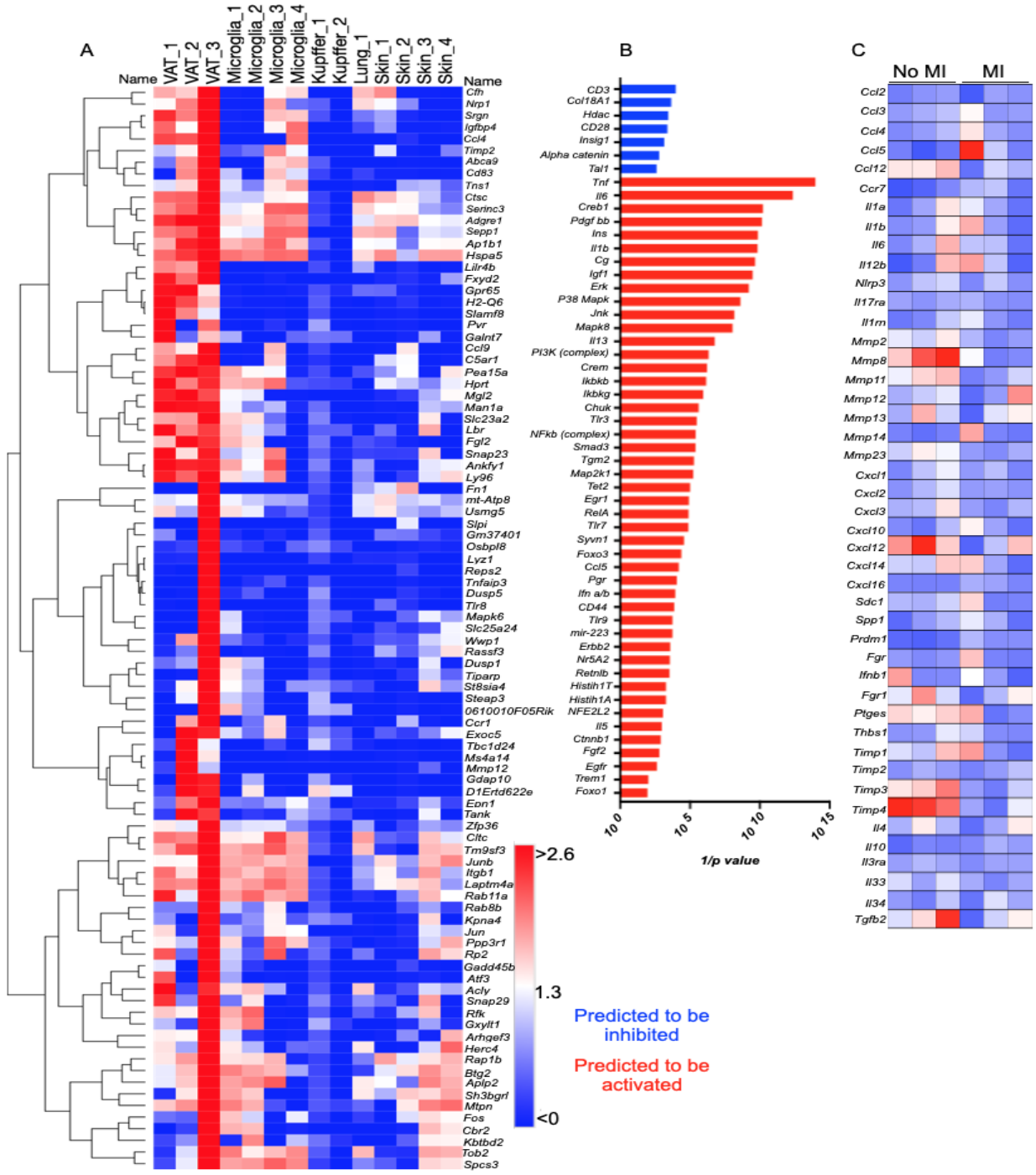

Fig. S7. VAT-resident macrophages are predicted to express genes involved in lipid metabolism and insulin sensitivity. All of these experiments were performed in lean C57BL/6 mice without (**A&B**) or with (**C**) MI. (**A**) The heat map shows the genes differentially expressed only in VAT resident macrophages compared to the other tissue resident macrophages. (**B**) After analyzing these genes using IPA, we identified VAT resident macrophage-specific signature genes, which are involved in lipid metabolism and insulin sensitivity. (**C**) CX_3CR1^{low} $CCR2^{low}$ VAT macrophages were isolated using fluorescent activated cell sorting from mice with or without MI. Whole genome RNA sequencing was performed and the list of the inflammatory genes were obtained using the Ingenuity Pathway Analysis. n=3 mice per group.

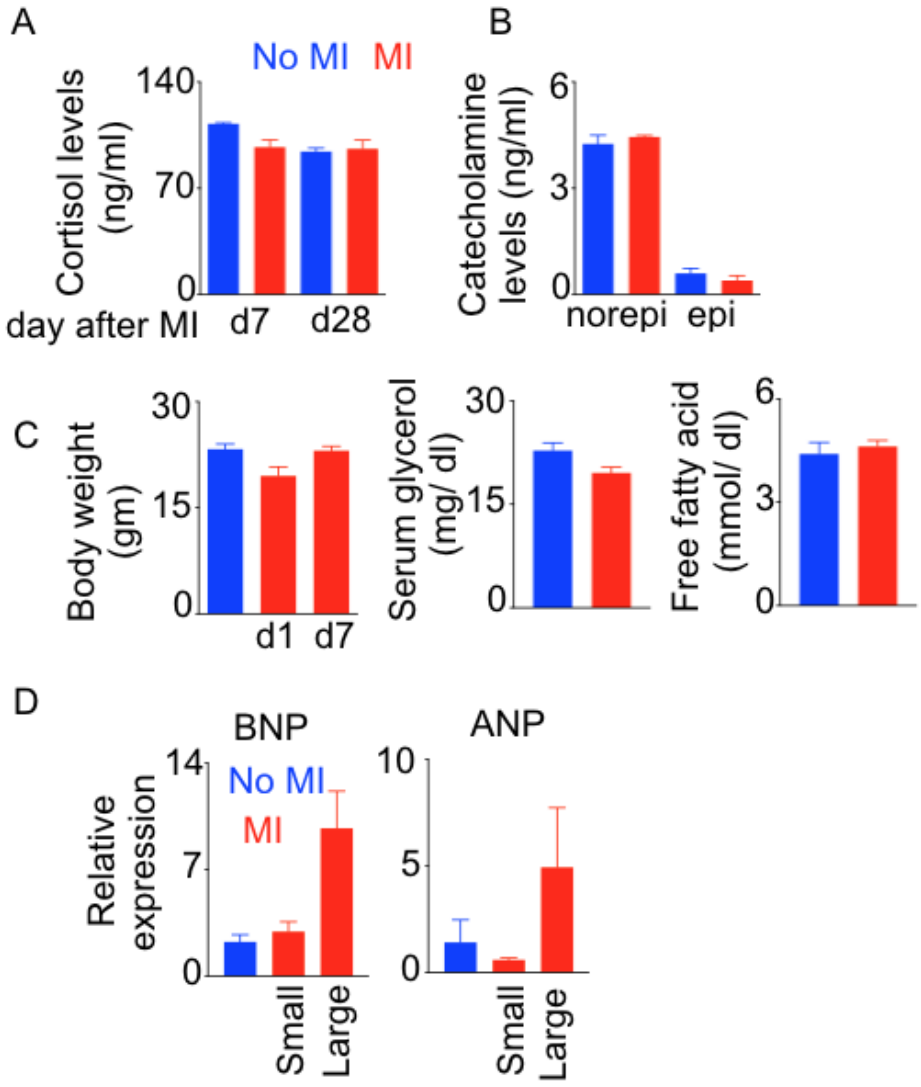

Fig. S8. Post-MI insulin resistance is not accompanied by increased contents of cortisol and catecholamine, lipolysis, or heart failure. All of these experiments were performed in lean C57BL/6 mice on day 1, 7 and 28 after MI. Quantification of serum cortisol at day 7 and 28 after MI (**A**) (n=3-4 per group) and catecholamine concentrations at day 7 after MI (**B**) (n=4 per group). (**C**) Body weights on day 1 and 7, and serum lipid contents on day 7 after MI. n=4-28 per group. (**D**) mRNA quantification of brain natriuretic peptide (BNP) and atrial natriuretic peptide (ANP), markers of heart failure, in the left ventricle at day 7 after MI. n=3-5 per group. Mean ± s.e.m.

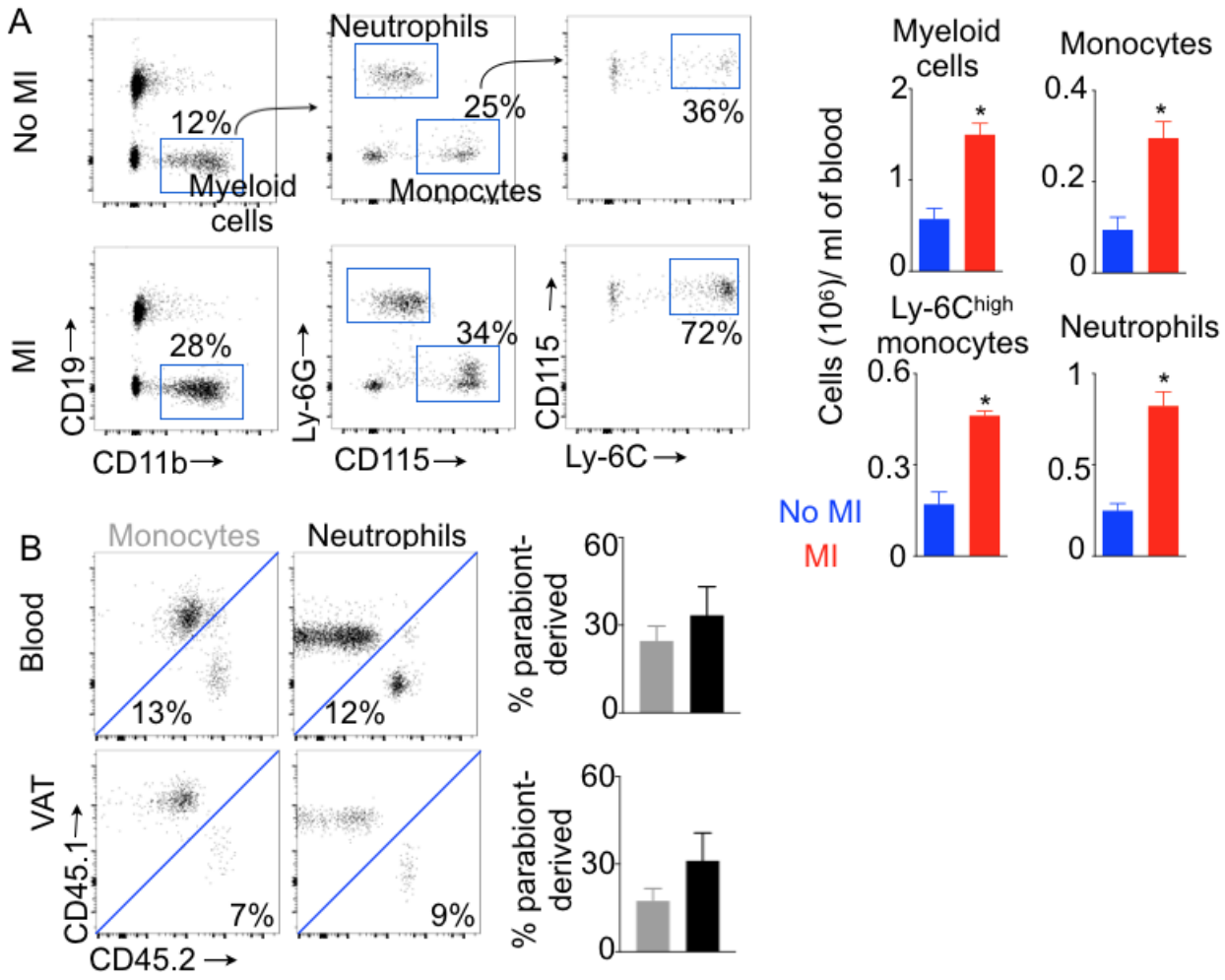

Fig. S9. MI increases the number of circulating myeloid cells. (A) The flow cytometric plots show the gating strategy for different myeloid cells in VAT. The bar plots depict myeloid cell numbers in the blood in lean C57BL/6 mice on day 7 after MI. n=5 per group. Data from one of two independently performed experiments are shown. n=3-5 per group. (**B**) The bar graphs show the amounts of monocyte and neutrophil chimerism in the blood and VAT of CD45.1 parabionts without MI. n=4 pairs. Mean ± s.e.m. * $P < 0.05$.

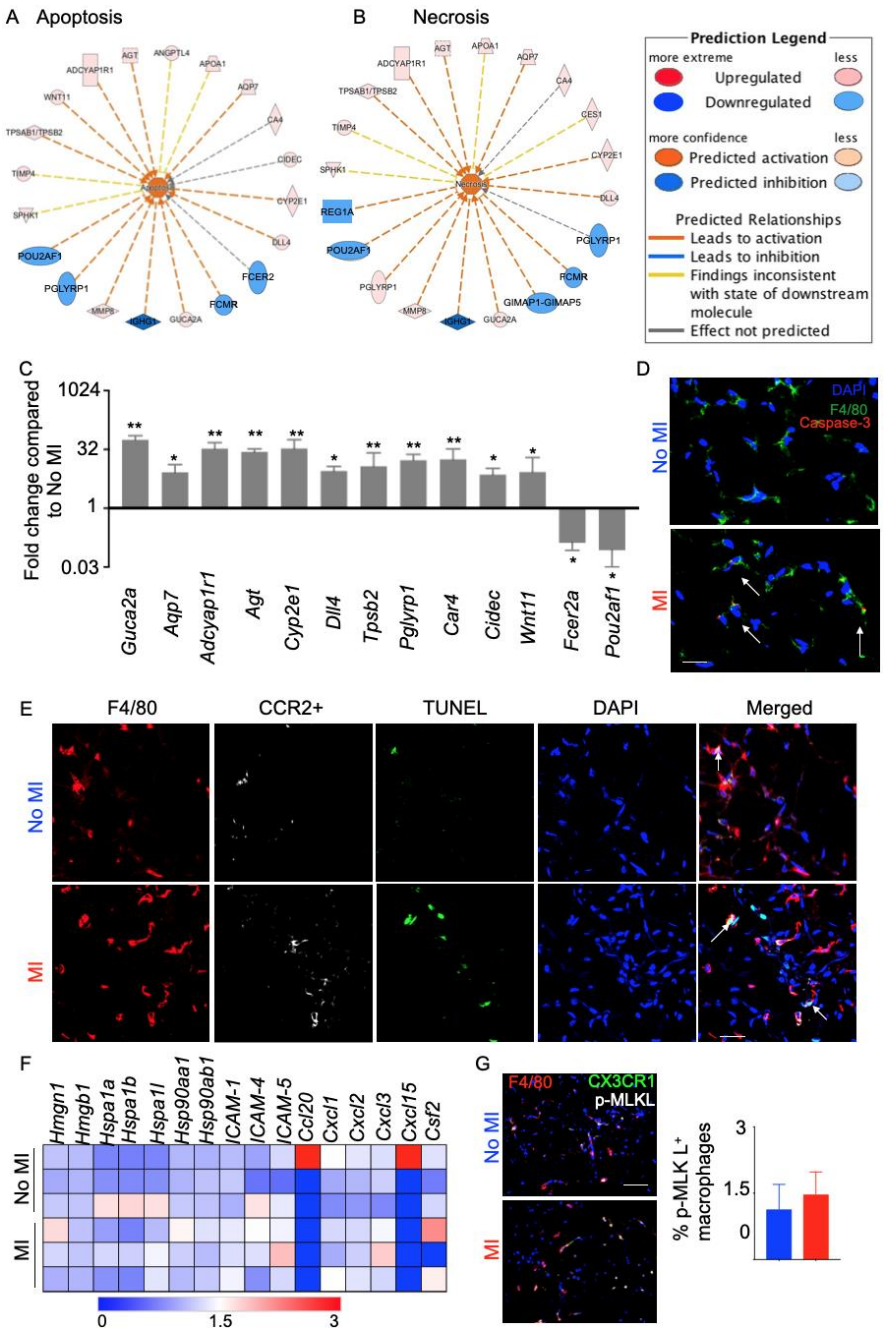

Fig. S10. Enrichment of genes involved in cellular apoptosis and necrosis in VAT-resident macrophages in C57BL/6 mice on day 7 after MI. The gene networks show the differentially expressed genes involved in apoptosis (**A**) and necrosis (**B**). These genes are enriched in VAT-resident macrophages isolated from mice on day 7 after MI. (**C**) qPCR confirmation of the expression of the genes involved in cellular apoptosis. n=4-6 per group. (**D**) Caspase 3 staining in VAT on day 7 after MI. Scale bar=10 μm. (**E**) TUNEL$^+$ apoptotic VAT resident macrophages were quantified using confocal microscopy in mice with or without MI. Scale bar=5 μm. (**F**) Expression of the genes reported to be increased in necroptotic cells and (**G**) pMLKL staining in VAT macrophages. Autofluorescent VAT resident macrophages were distinguished from non-autofluorescent monocyte-derived macrophages. Scale bar=10 μm. n=6 mice per group. Mean ± s.e.m. * P<0.05, **P<0.01.

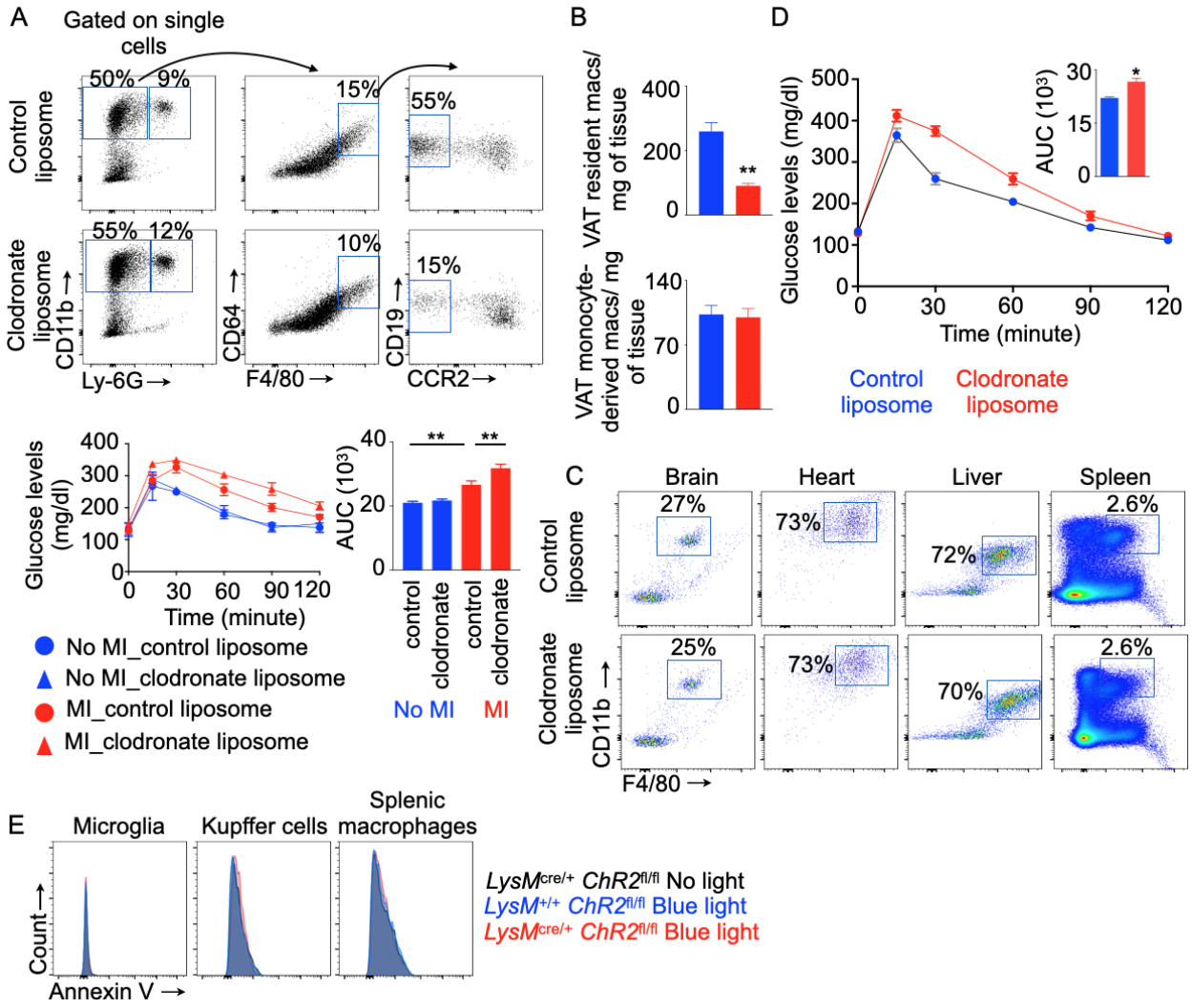

Fig. S11. Depletion of VAT-resident macrophage exacerbates glucose intolerance on day 7 after MI. (**A**) The upper panel depicts flow cytometric gating strategy showing different myeloid populations in mice treated with either control or clodronate liposome. Lean C57BL/6 mice with or without MI were injected i.p with either control or clodronate liposome on the day of the surgery. An intraperitoneal glucose tolerance test was performed on day 7 after the surgery. n=5-8 mice per group. (**B-D**) Control or clodronate liposome was directly injected in epididymal adipose tissue. (**B**) Quantification of the VAT macrophage subsets after clodronate or control liposome treatment. n=4 per group. (**C**) Representative flow cytometric plots show macrophages in various organs. n=5 per group. (**D**) A glucose tolerance test was performed. n=4-5 mice per group. (**E**) Annexin V expression was measured in VAT-resident macrophages in lean control and *LysM*$^{cre/+}$ *ChR2*$^{fl/fl}$ mice without MI after 20 minutes of blue light exposure. Mean ± s.e.m. *P < 0.05, **P<0.01.

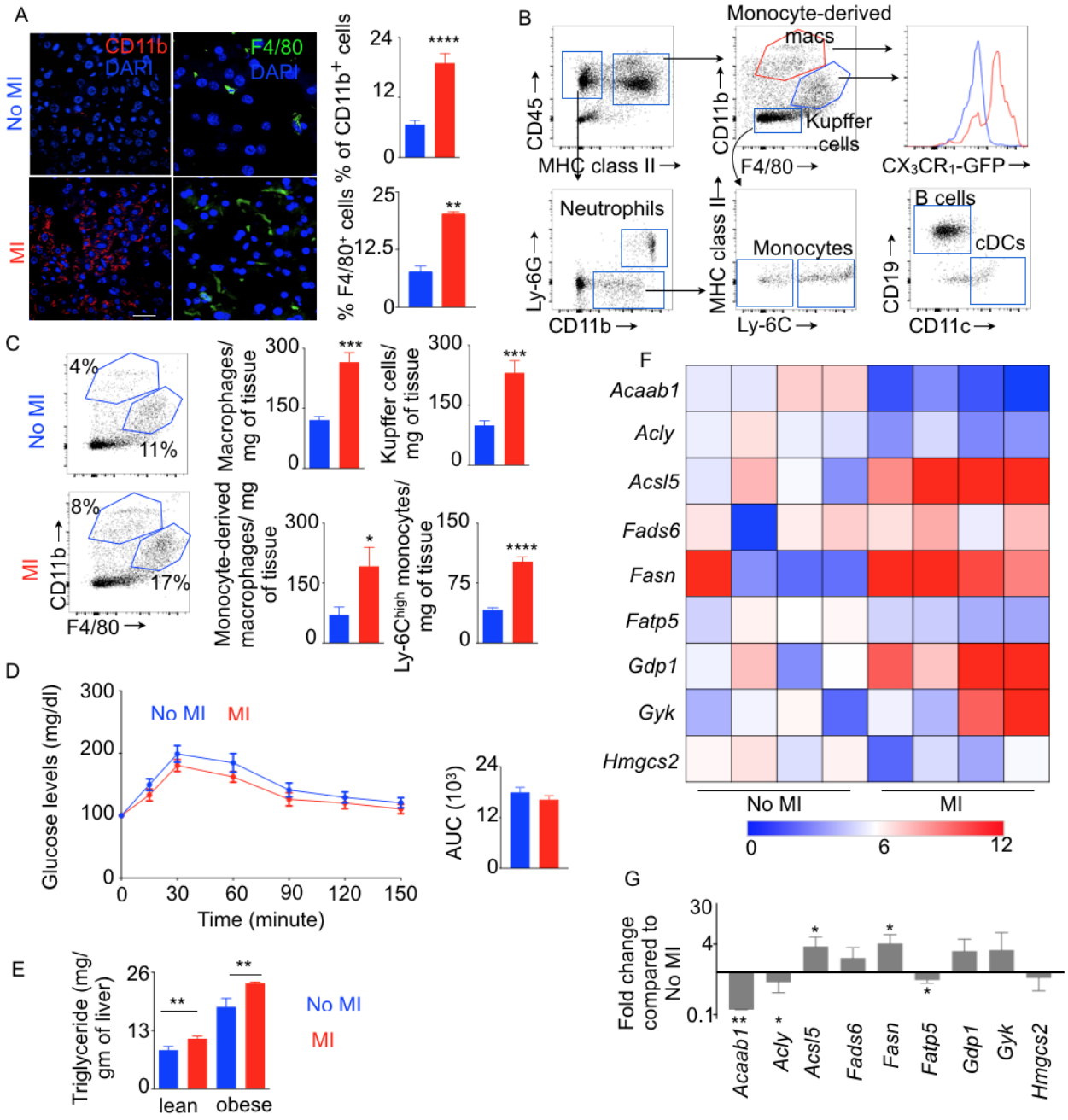

Fig. S12. MI alters hepatic metabolism. All of these experiments were performed in either lean or obese C57BL/6 or *Cx3cr1*$^{+/gfp}$ mice on day 7 after MI. (**A**) Confocal images show CD11b^{+} and F4/80^{+} cells in the liver. Scale bar=20 μm. n=9 per group. (**B**) Gating strategy for various leukocytes in the liver. (**C**) Quantification of hepatic leukocyte subsets using flow cytometry. n=8-9 per group. Pyruvate tolerance test in lean mice. n=5 per group. (**D**) and hepatic triglyceride contents (**E**) in lean and obese mice after MI (n=3-4 per group). The heatmap (**F**) and bar plots (**G**) show the expression of genes involved in lipid metabolism in the liver. n=4-5 per group. Data were derived from at least two independently performed experiments. Mean ± s.e.m. * $P < 0.05$, ** $P < 0.01$, *** $P < 0.001$.

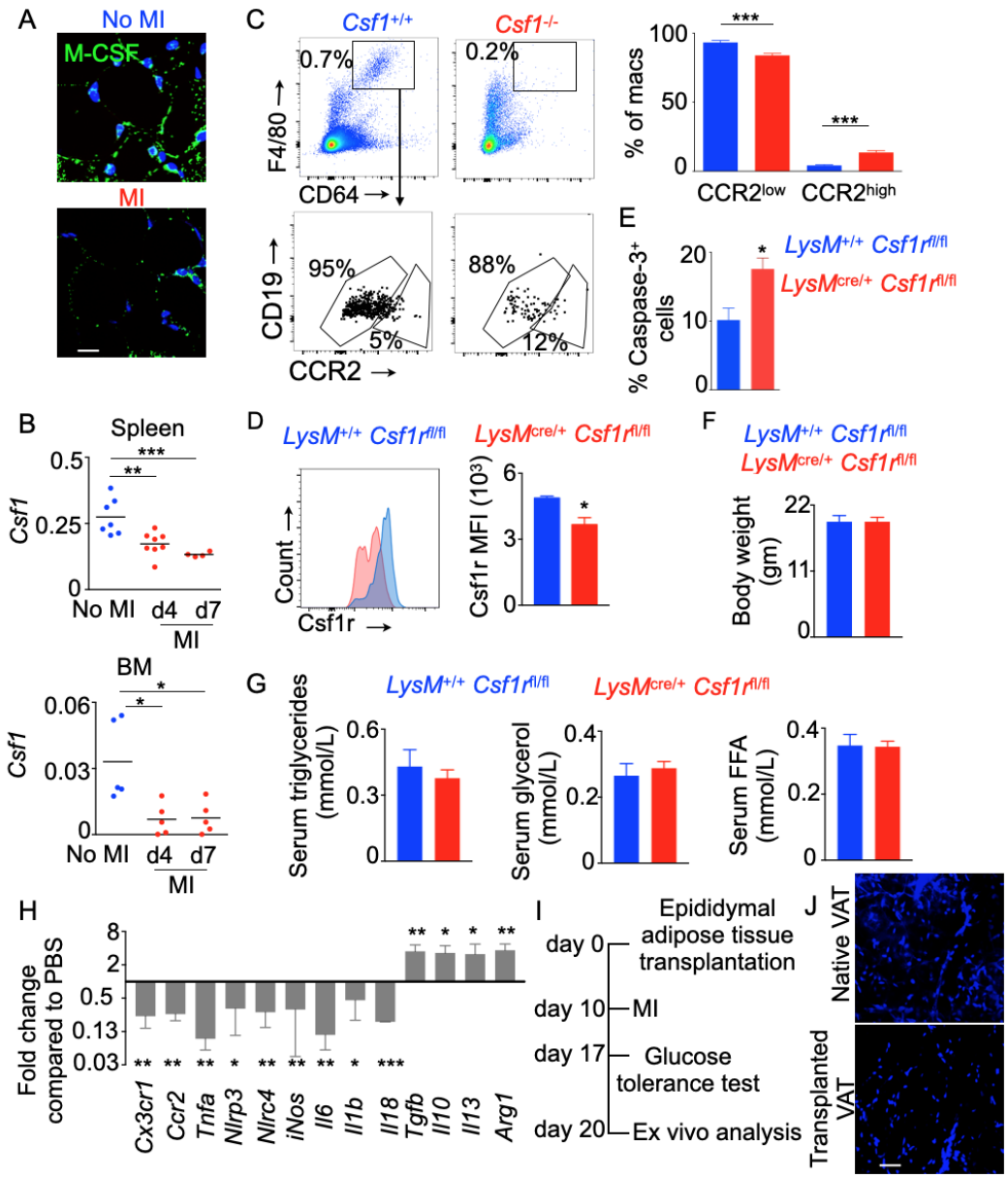

Fig. S13. Csf1-deficient mice have reduced number of VAT-resident macrophages. All of these experiments were performed in lean transgenic mice on C57BL/6 background with or without MI. Csf1 was measured in VAT (**A**), and spleen and bone marrow (**B**) (n=4-8 per group) in lean C57BL/6 mice on day 7 after MI by confocal microscopy and qPCR, respectively. Scale bar=50 μm. (**C**) Enumeration of the VAT macrophage subsets in *Csf1*$^{+/+}$ and *Csf1*$^{-/-}$ (op/op) mice without MI. n=5-9 per group. The data are pooled from four independently performed experiments. (**D**) Csf1r expression in VAT-resident macrophages (n=4-5 per group) and (**E**) enumeration of caspase 3^{+} VAT-resident macrophages (n=4-5 per group) in *LysM*$^{+/+}$ *Csf1r*$^{fl/fl}$ and *LysM*$^{cre/+}$ *Csf1r*$^{fl/fl}$ mice on day 7 after MI. Body weight (**F**) (n=6-10 per group) and serum lipid concentrations (**G**) (n=3-9 per group) in these mice on day 7 after MI. (**H**) qPCR quantification of pro- and anti-inflammatory genes in sorted VAT-resident macrophages in C57BL/6 mice after Csf1 supplementation on day 7 after MI. n=4 per group. (**I**) Experimental design for adipose tissue transplantation. (**J**) Native and transplanted VAT sections were stained with DAPI. Scale bar=30 μm. n=4-9 per group. Mean ± s.e.m. * $P < 0.05$, *** $P < 0.001$.

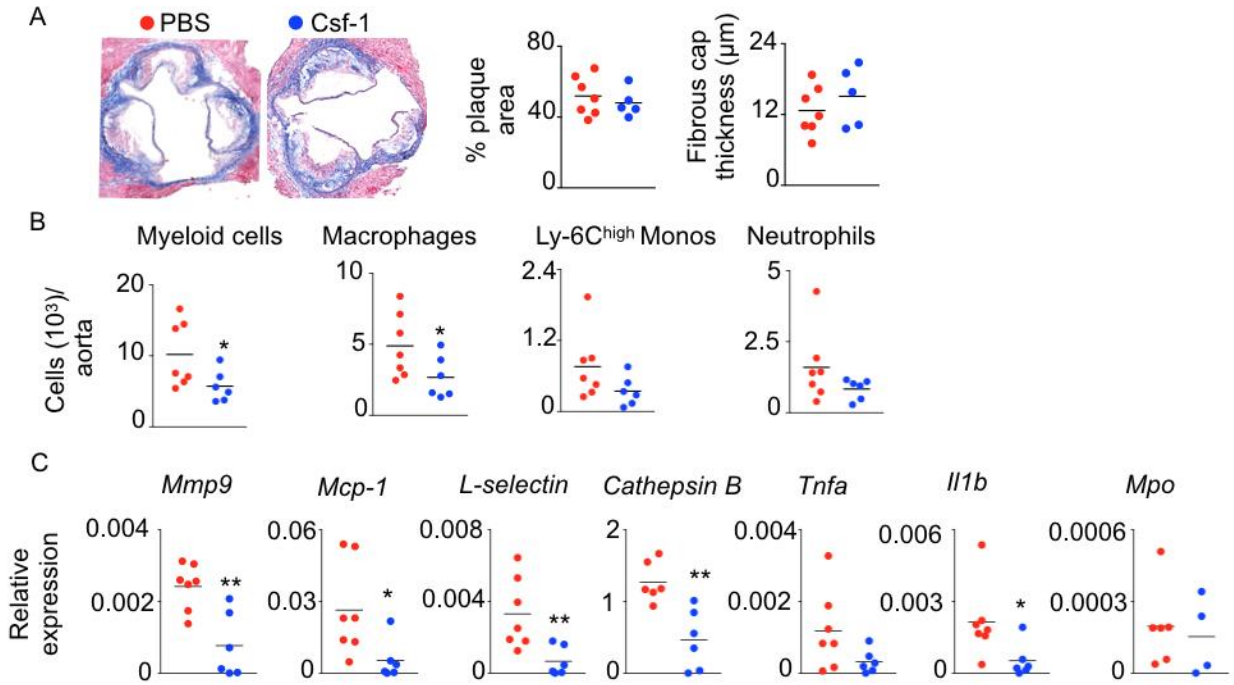

Fig. S14.Csf1 supplementation in *Apoe*$^{-/-}$ mice after MI decreases atherosclerotic plaque inflammation without affecting atherosclerotic plaque size. *Apoe*$^{-/-}$ mice fed an atherogenic diet were infused with Csf1 for four days after MI. Ex vivo analyses were performed four months later. (**A**) Quantification of atherosclerotic plaque areas with Masson's trichrome staining. n=5-7 per group. (**B**) Enumeration of inflammatory myeloid cell subsets in the aorta with flow cytometry. n=6-7 per group. (**C**) Quantification of genes encoding inflammatory cytokines and cathepsin B in the aortic arch using qRT-PCR. n=6-7 per group. Mean ± s.e.m. * $P < 0.05$, ** $P < 0.01$.

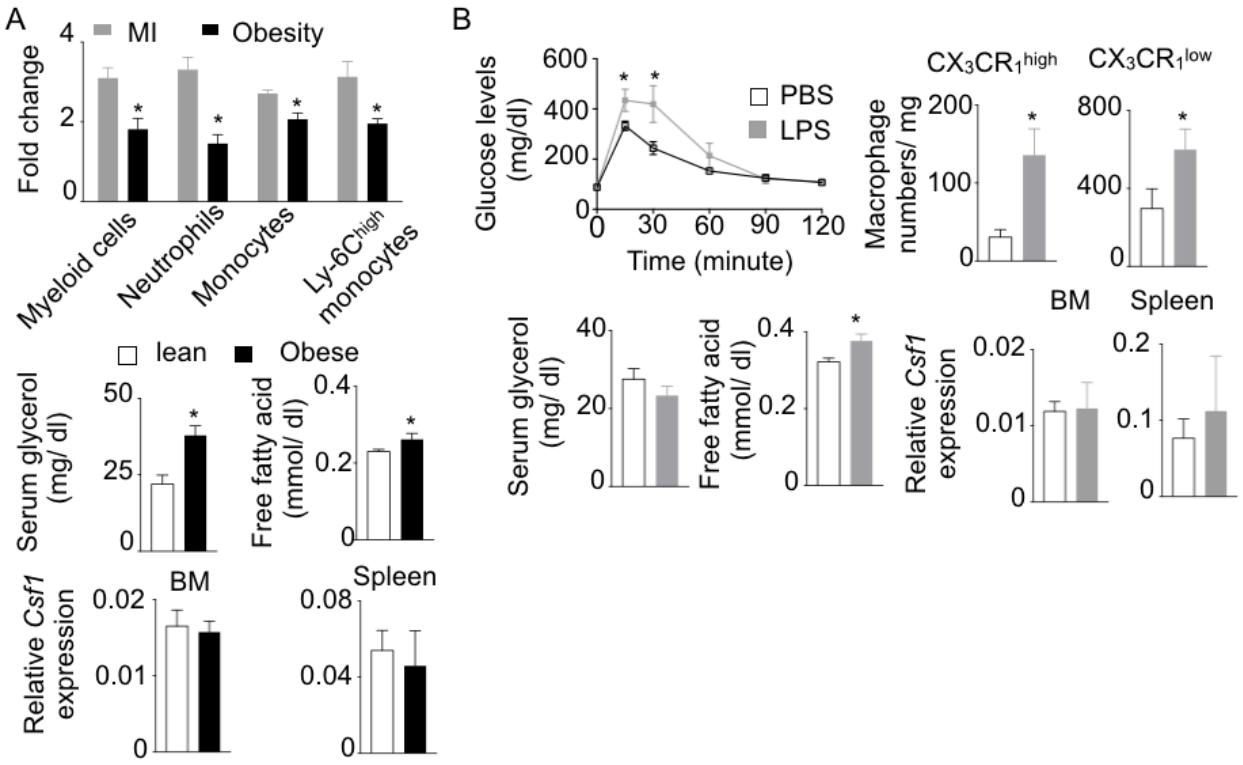

Fig. S15. MI-induced insulin resistance is unique compared to other causes of insulin resistance. (**A**) The upper panel shows fold changes in various myeloid cell subsets in obese C57BL/6 mice without MI and lean C57BL/6 mice with MI compared to respective controls. For MI, mice with sham surgery and for obesity, lean mice were used as controls. The middle panels depict serum glycerol and free fatty acid concentrations in obese mice compared to lean control mice. The lower panels show quantification of *Csf1* in lean and obese mice. n=3-5 per group. (**B**) The upper panels show GTT and quantification of VAT macrophage subsets in lean C57BL/6 mice injected with either PBS or LPS. The lower panels show serum glycerol and free fatty acid contents, and relative *Csf1* expression in the bone marrow and spleen of these mice. n=4-6 per group. Mean ± s.e.m. * $P < 0.05$.

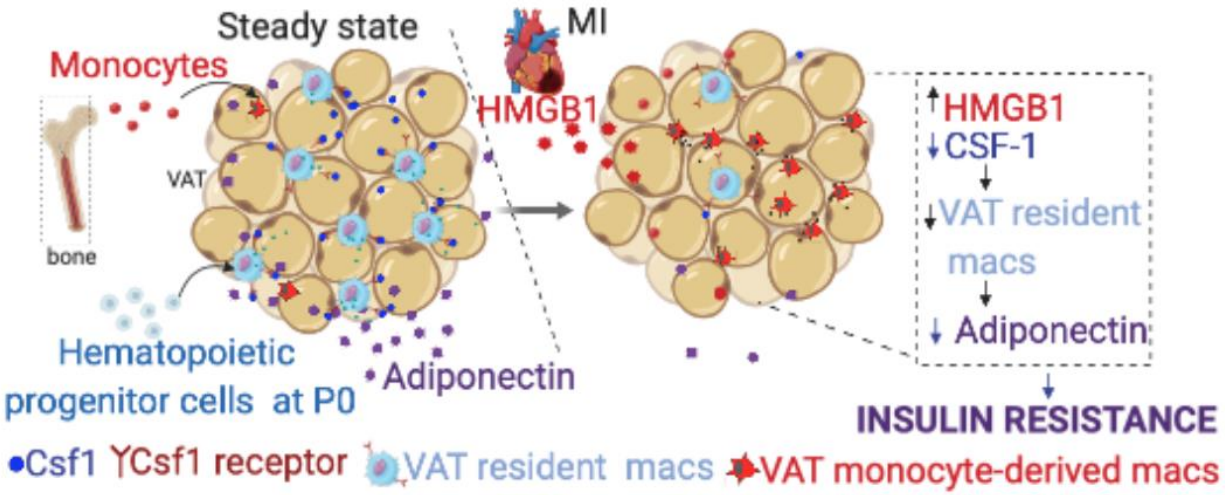

Fig. S16. Schematic depicting potential mechanisms of MI-induced insulin resistance.

Table S1. Demographics of patients with STEMI. The table shows age, gender, BMI, medicines, pre-MI glucose concentrations (mg/dL, 15 days before STEMI), post-MI glucose contents (30 days after STEMI), and diagnosis of diabetes, hypertension and dyslipidemia in patients with ST-elevation myocardial infarction. n=27.

Patient #	Pre-MI glucose	Post-MI glucose	Age	Gender	Diabetes	Hypertension	Dyslipidemia	BMI	ACEi	Statin	Beta Blocker
1	105	103	88	F	No	Yes	Yes	26	Yes	Yes	Yes
2	86	97	59	M	No	Yes	Yes	34	No	Yes	Yes
3	84	102	90	M	No	Yes	Yes	25	Yes	Yes	Yes
4	92	95	69	M	No	Yes	No	36	Yes	Yes	Yes
5	95	88	53	M	No	No	Yes	30	No	Yes	Yes
6	95	101	58	M	No	Yes	No	27	No	Yes	Yes
7	114	104	63	M	No	Yes	No	33	Yes	Yes	Yes
8	100	102	59	F	No	Yes	Yes	18	No	Yes	No
9	119	109	55	M	No	Yes	Yes	35	Yes	Yes	Yes
10	97	100	73	M	No	Yes	Yes	24	No	Yes	Yes
11	102	90	58	M	No	Yes	No	29	Yes	Yes	Yes
12	82	97	62	F	No	Yes	No	41	No	Yes	Yes
13	101	101	61	M	No	No	Yes	24	Yes	Yes	Yes
14	110	256	62	M	No	Yes	Yes	40	No	Yes	Yes
15	90	111	50	M	No	Yes	No	27	No	Yes	Yes
16	110	132	59	F	No	Yes	No	24	No	Yes	Yes
17	91	114	61	M	No	No	Yes	22	No	Yes	Yes
18	120	203	84	F	No	Yes	Yes	22	Yes	Yes	Yes
19	105	112	58	M	No	Yes	Yes	26	Yes	Yes	Yes
20	103	207	77	F	No	No	No	19	Yes	Yes	Yes
21	106	119	44	M	No	Yes	Yes	25	Yes	Yes	Yes
22	110	154	59	M	No	No	Yes	28	Yes	Yes	Yes
23	97	215	71	M	No	Yes	Yes	26	Yes	Yes	Yes
24	104	115	64	F	No	No	No	25	No	Yes	Yes
25	114	234	69	M	No	Yes	Yes	34	No	Yes	Yes
26	113	127	59	F	No	Yes	Yes	22	Yes	Yes	Yes
27	110	124	64	F	No	Yes	Yes	37	Yes	Yes	Yes

Table S2. The primer sequences for the genes used in the qPCR experiments.

Gene	Sequence	Source
Acaab1	CAG GAC GTG AAG CTA AAG CCT-F CTC CGA AGT TAT CCC CAT AGG AA-R	IDT
Acly	CCA AGG CAA TTT CAG AGC AGA-F CAG AGA GAG ATT GAC CCC GAC-R	IDT
Acsl5	AAC CAG TCT GTG GGG ATT GAG-F CGT CTT GGC GTC TGA GAA GTA-R	IDT
Adcyap1r1	CTG CGT GCA GAA ATG CTA CTG-F AGC CGT AGA GTA ATG GTG GAT AG-R	IDT
Agt	TCT CCT TTA CCA CAA CAA GAG CA-F CTT CTC ATT CAC AGG GGA GGT-R	IDT
ANP	GAG AAG ATG CCG GTA GAA GA-F AAG CAC TGC CGT CTC TCA GA-R	IDT
Aqp7	AAT ATG GTG CGA GAG TTT CTG G-F ACC CAA GTT GAC ACC GAG ATA-R	IDT
Arginase	GTG GCT TTA ACC TTG GCT TG-F CTG TCT GCT TTG CTG TGA TG-R	IDT
Beta-actin	GGC TGT ATT CCC CTC CAT CG-F CCA GTT GGT AAC AAT GCC ATG T-R	IDT
BNP	CTG CTG GAG CTG ATA AGA GA-F TGC CCA AAG CAG CTT GAG AT-R	IDT
Car4	TAC GTG GCC CCC TCT ACT G-F GCT GAT TCT CCT TAC AGG CTC C-R	IDT
CCR2	ATC CAC GGC ATA CTA TCA ACA TC- F CAA GGC TCA CCA TCA TCG TAG-R	IDT
Cidec	ATG GAC TAC GCC ATG AAG TCT-F CGG TGC TAA CAC GAC AGG G-R	IDT
CSF-1	ATG AGC AGG AGT ATT GCC AAG G-F TCC ATT CCC AAT CAT GTG GCT A-R	IDT
Csf1R	TGT CAT CGA GCC TAG TGG C-F CGG GAG ATT CAG GGT CCA AG-R	IDT
CX3CR1	GAG TAT GAC GAT TCT GCT GAG G-F CAG ACC GAA CGT GAA GAC GAG -R	IDT
Cyp2E1	CGT TGC CTT GCT TGT CTG GA-F AAG AAA GGA ATT GGG AAA GGT CC-R	IDT

DII4	TTC CAG GCA ACC TTC TCC GA-F ACTGCCGCTATTCTTGTCCC-R	IDT
Fads6	AGC ACA TCG GAC TGC CTA TG-F TCG TGG AGA AAC TTC GAC ACC-R	IDT
Fasn	AGA GAT CCC GAG ACG CTT CT-F GCT TGG TCC TTT GAA GTC GAA GA-R	IDT
Fatp5	GTT CTC CCG TCC AAG ACC ATT-F GCT CCG TAC AGA GTG TAG CAA G-R	IDT
Fcer2a	CCA GGA GGA TCT AAG GAA CGC - F TCG TCT TGG AGT CTG TTC AGG -R	IDT
Gpd1	CCA TGT GGG TGT TTG AGG AAG-F GCC CTG GCA GGT ATT TAA CAT TC-R	IDT
Guca2a	CCC AGA CTG GTG AGT CAC AAG-F GCG TTG GGT TTC TCG CAG A-R	IDT
Gyk	TGG GTA GAA CAA GAC CCG AAG-F GTT GCT GAC ACC AAT GGC TT-R	IDT
GAPDH	TGT AGA CCA TGT AGT TGA GGT CA-F AGG TCG GTG TGA ACG GAT TTG-R	IDT
Hmgcs-2	AGA GAG CGA TGC AGG AAA CTT-F AAG GAT GCC CAC ATC TTT TGG-R	IDT
IL-1beta	GCA ACT GTT CCT GAA CTC AAC T-F ATC TTT TGG GGT CCG TCA ACT-R	IDT
IL-6	TAG TCC TTC CTA CCC CAA TTT CC-F TTG GTC CTT AGC CAC TCC TTC-R	IDT
IL-10	GCT CTT ACT GAC TGG CAT GAG-F CGC AGC TCT AGG AGC ATG TG-R	IDT
IL-13	GGA GCG AAT GGA GTG AAG AGG-F GCT CAA TGT GGG TTC AGG TTC-R	IDT
IL-18	GTT CAC TCT CAC TAA CTT ACA TCA AAG-F TCT ATA AAT CAT GCA GCC TCG G-R	IDT
iNOS	TTG CTC ATG ACA TCG ACC AG-F ACA TCA AAG GTC TCA CAG GC-R	IDT
NLRC4	AGT ATG ATA GTC TTT GGC CTT CC-F TGA ATA AGG GCT CGT CTG TTG-R	IDT
NLRP-3	CTC CAA CCA TTC TCT GAC CAG-F ACA GAT TGA AGT AAG GCC GG-R	IDT
Pglyrp1	GCC ATC CGA GTG CTC TAG C-F	IDT

	CTT GTG GTA ATG CTG CAC ATT G-R	
Pou2af1	CAC CAA GGC CAT ACC AGG G-F GAA GCA GAA ACC TCC ATG TCA-R	IDT
TGF-beta	CCT GAG TGG CTG TCT TTT GA-F CGT GGA GTT TGT TAT CTT TGC TG-R	IDT
TNF-alfa	CTT CTG TCT ACT GAA CTT CGG G-F CAG GCT TGT CAC TCG AAT TTT G-R	IDT
TPSB2	CTG GCT AGT CTG GTG TAC TCA-F CAG GGC CAC TTA CTC TCA GAA-R	IDT
Wnt11	GCT GGC ACT GTC CAA GAC TC-F CTC CCG TGT ACC TCT CTC CA-R	IDT

Movies S1 and S2. MI decreases the frequency of VAT-resident macrophages. Intravital microscopy showing VAT macrophage subsets in lean $CX_3CR1^{CreER/+}$ $ROSA^{tdTomato/+}$ mice without (**Movie S1**) or with (**Movie S2**) MI (day 7). These mice were injected with tamoxifen on five consecutive days before intravital microscopy. CX_3CR1^{high} $CCR2^{high}$ and CX_3CR1^{low} $CCR2^{low}$ VAT macrophages are red and green, respectively.